Markov Chain Signal Generation based on Single Magnetic Tunnel Junction

Xihui Yuan, Jiajia Jian, Zheng Chai, Suihuan An, Yawei Gao, Xue Zhou, Jian Fu Zhang, Weidong Zhang and Tai Min

***Abstract*—Markov chain (MC) is a stochastic model that describes a sequence of events where the probability of each event depends only on the previous state. Such memoryless property makes MC widely used in machine learning and encryption, but the hardware implementation of MC generation remains challenging. This paper presents a hardware solution for generating MC signals using only one industry-ready magnetic tunnel junction (MTJ). High quality standard MC signal has been generated with low error and good randomness. The proposed solution also demonstrates the potential in increasing the generation speed. The presented solution offers a hardware-friendly implementation of MC signal in semiconductor chips.**

***Index Terms*—Markov chain, magnetic tunnel junction, probabilistic switching, spintronic devices**

I. Introduction

MARKOV chain (MC), a fundamental mathematical model, describes random systems in which the future states can be predicted based only on the present states regardless of the past [1]-[3]. Such memoryless property of MC has been widely exploited in machine learning and encryption. However, the practical MC generation is still based on software [4], while the hardware implementation remains challenging. In scaled semiconductor devices, the random telegraph noise (RTN), induced by the carrier capture/emission of single random defect [5] [6], is a MC signal [7]-[9]. However, extracting MC signal from RTN is not easy, because large device arrays are needed to pick one device with clear RTN [7], and that has to be done manually or with complex algorithms [10] [11].

Recently, the probabilistic switching property of emerging devices has been attractive for the stochasticity-related applications, such as Boltzmann machines [12] [13] and spiking neural networks (SNNs) [14] [15]. Previous work reported the generation of MC signal using a dual-layered SnSe-based RRAM, exploiting its probabilistic switching [16]. However, the device is yet far from commercialization, and its endurance is very limited.

Spintronic devices, such as the spin torque transfer magnetic random access memory (STT-MRAM) [17]-[20], the spin orbit transfer (SOT)-MRAM [21] and the domain wall Hall cross-bars [22], have been used to generate random bits. Typically, in each bit-generation cycle, a pulse probabilistically switches the device, a read pulse gets the device state, and a deterministic pulse reset the device. This is like a coin toss: the outcome of each cycle is independent from all the others, including the previous one. In mathematics, the generated random bit stream is a sequence of independent random variables, which is technically not a standard MC where the probability of each event depends only on the state attained in the previous event. [23] and [24] generate telegraphic switching signal in MRAM devices, using both magnetic fields and electrical pulse, which are difficult to implement in IC chips.

In this paper, we present a hardware solution for generating MC signals. The core device is an industry-ready magnetic tunnel junction (MTJ) which is operated by a specially designed three-pulse waveform. High quality standard MC signal has been generated with low error and good randomness. The proposed solution also shows potential for high-speed generation. The presented solution offers a hardware-friendly way to generate MC signal in semiconductor chips, for the emerging applications.

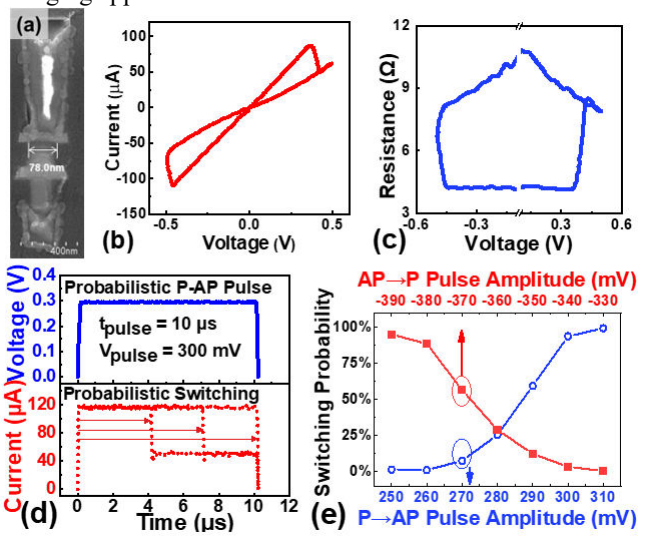

Fig.1. (a) Cross-section SEM image of the MTJ, whose (b) I-V and (c) R-V curves demonstrate the magneto-resistive switching. The stochastic switching demonstrated in (d) shows (e) sigmoid-like dependence of switching probability on pulse amplitude in both polarities, with a fixed pulse width of 10 μs.

Manuscript received xx. This work is supported by the National Key R&D Program of China (Grant No. 2022YFB4400200), the National Natural Science Foundation of China (Grant No. 62104188), and in part by the major key project of Peng Cheng Laboratory under grant PCL2023AS1-2. (Corresponding author: Zheng Chai, Tai Min.)

Xihui Yuan, Jiajia Jian, Zheng Chai, Suihuan An, Yawei Gao, Xue Zhou, and Tai Min are with the Center for Spintronic and Quantum Systems, State Key Laboratory for Mechanical Behavior of Materials, and School of Materials Science and Engineering, Xi'an Jiaotong University, Xi'an, China, and also with the Peng Cheng Laboratory, Shenzhen, Guangdong 518055, China, and also with the Pazhou Laboratory (Huangpu), Guangzhou, Guangdong 510555, China (e-mail: zheng.chai@xjtu.edu.cn, tai.min@mail.xjtu.edu.cn).

Jian Fu Zhang and Weidong Zhang are with the School of Engineering, Liverpool John Moores University, L3 3AF Liverpool, U.K.(e-mail: w.zhang@ljmu.ac.uk)

II. Device and Experiment

The core device to generate MC signal is a bottom pinned perpendicular magnetization anisotropy (PMA) MTJ with diameter around 70 nm. Its cross-sectional scanning electron microscopy (SEM) is presented in **Fig. 1a**. The magneto-resistive switching between the parallel (P) and anti-parallel (AP) states is demonstrated in the I-V and corresponding R-V plot in **Fig. 1b&c** respectively, with a tunnel magnetoresistance (TMR) of ~200%. All electrical measurements were conducted using the pulse measurement units (PMUs) in a Keithley 4200 semiconductor characterization system.

III. Results and Discussions

The probabilistic switching of MTJ is demonstrated in **Fig. 1d**: During a voltage pulse, the MTJ may either switch or remain un-switched. Such probabilistic switching exists in both voltage polarities, with sigmoid-like dependence between the switching probability and pulse amplitude (**Fig. 1e**), which can be explained by the Néel Brown model [25]:

$$P(t) = 1 - exp(-t/\tau) \quad (1)$$

where $P(t)$ is the thermal switching probability, and τ is the relaxation time:

$$\tau = f_0^{-1} exp(E_b/k_B T) \quad (2)$$

where f_0 is the attempt frequency, E_b is the energy barrier, and T is the temperature.

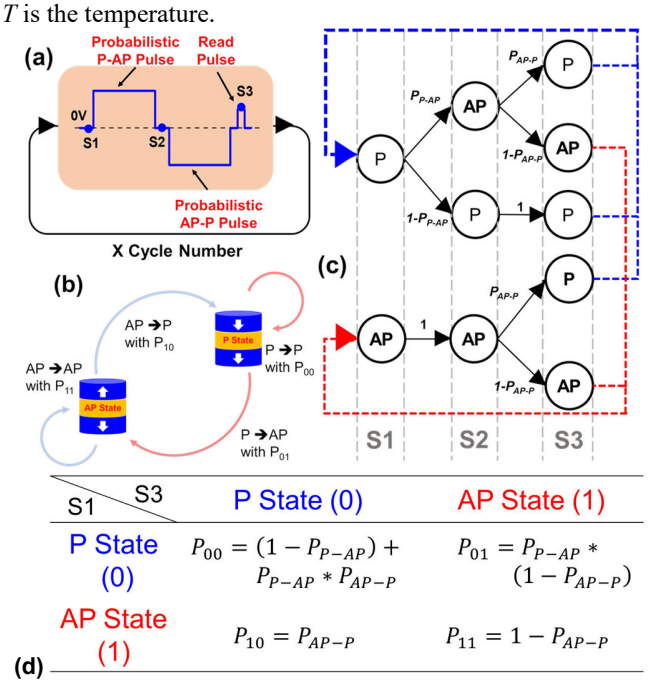

Fig.2. (a) Schematic of the three-pulse waveform. (b) Schematic of state transition. (c) When S1 is at P/AP state, the resulted S2 and S3 with corresponding probabilities. (d) State transition matrix of S1 and S3 in one cycle. P is defined as 0 and AP as 1; e.g., P_{00} means the probability of S3 = P (or 0) when S1 = P (or 0).

For a preliminary demonstration of the MC generation solution, 10,000 cycles are repeatedly applied onto the top electrode of the MTJ, with its bottom electrode grounded, to generate 10,000 bits. Each cycle has a three-pulse waveform (**Fig. 2a**) comprising a pulse for probabilistic P-to-AP transition, a pulse for probabilistic AP-to-P transition, and a read pulse. The states before the first and second pulse are named as S1 and S2, respectively. Current measurement is only carried out by the read pulse to get S3. S3 obtained from all cycles form a sequence, which is the generation result. Note that the S3 in one cycle is practically the same as the S1 in the next cycle, due to the non-volatility of the MTJ.

Regarding the relation between the S3 in one cycle and the next cycle, there are 4 cases: (1) AP → AP; (2) P → P; (3) AP → P; (4) P → AP, as summarized in **Fig. 2b**. **Fig. 2c** schematizes the resulted S2 and S3 with the corresponding probabilities. Since each S3 in the MC is influenced by, and only influenced by the S1 in the same cycle (that is, S3 in the last cycle), the generated bit stream conforms to the definition of a standard MC. This is further evidenced by **Fig. 2d,** which is the state transition matrix of the generated result. Apparently, the different rows in the transition matrix support that the generated bits are not independent random variables.

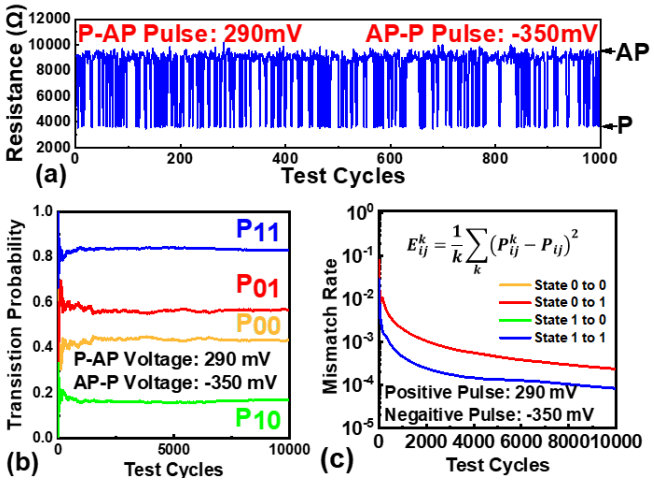

Fig.3. (a) MC signal generated at $V_{P\text{-}AP}$ =290 mV and $V_{AP\text{-}P}$ = -350mV. (b) The state transition probabilities approach to the steady values with the cycle number. (c) The mismatch rate gradually decreases after more cycle. The E_{11} and E_{01} overlap with the E_{10} and E_{00}, respectively.

Next, the quality of the generated MC signal is evaluated following the multiple steps [16]:

(i) The transition probabilities during the 10,000 cycles are calculated using Equation (3):

$$P_{ij}^k = \frac{n_{ij}^k}{n_{ii}^k + n_{ij}^k} \quad (i,j = 0/1) \quad (3)$$

where P_{ij}^k is the state transition probabilities (the probability transfer from state i to state j in the k cycles), k is the cycle number, and n_{ij}^k refers to the amount transfer from state i to state j in the k cycles.

(ii) The obtained transition probabilities are used to calculate the frequency distribution of AP state and P state, based on Equation (4) and (5):

$$\pi_P + \pi_{AP} = 1 \quad (4)$$

$$[\pi_P \quad \pi_{AP}]\, A = [\pi_P \quad \pi_{AP}] \quad (5)$$

where π_{AP} and π_P are the frequency distribution of AP state and P state, and A is the state transition matrix. π_{AP} and π_P are the eigenvector of A when the eigenvalue of A is 1.

(iii) Meanwhile, the experimental values of π_{AP} and π_P, are counted directly from the cycling results (e.g. **Fig. 3a**).

(iv) The calculated values of π_{AP} and π_P are compared to the counted values: the lower the relative error, the higher the generation quality.

Taking the MC generated at $V_{P\text{-}AP}$ =290 mV and $V_{AP\text{-}P}$ = -350mV (**Fig. 3a**) as example. Along with cycling, all state transition probabilities P_{ij}^k approach their steady values, P_{ij} (**Fig. 3b**), as evidenced by the decreasing mismatch rates between P_{ij}^k and P_{ij} for all transition probabilities (**Fig. 3c**). **Fig. 4a** and **Fig. 4b** summarize the π_{AP} and π_P with different combinations of pulse amplitude: the AP/P state's frequency distribution of the generated MC increases/decreases with a higher $V_{P\text{-}AP}$/a lower $V_{AP\text{-}P}$. Compared with the counted values, the calculated frequency distributions are quite close, with an averaged relative error of only 0.012% for AP state and 0.006% for P state, while their maximum values are 0.064% and 0.023%, respectively.

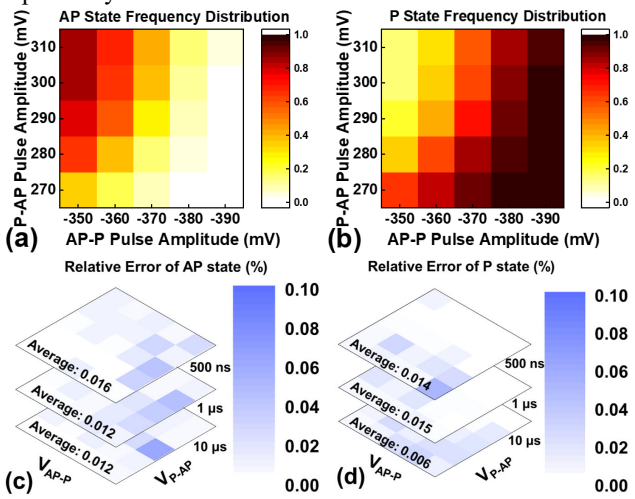

Fig.4. (a-b) Summary of the counted π_{AP} and π_P, when the pulse width is 10 µs. (c-d) The relative error between counted and calculated frequency distribution with pulse width scaling from 10 µs to 500 ns.

Furthermore, if pulse width is scaled from 10 µs to 500 ns, with adjusted pulse amplitude (**Fig. 4c&d**), high-quality MC could still be generated. As MTJ could be switched in the sub-ns regime [26], it could be safely estimated that the time per bit could be scaled to the nanosecond level, together with significant energy reduction. In addition, since MTJ is already industry-ready, and the waveform can be realized with clock/phase lock loop (PLL) circuits that are already used in every memory chip, this solution is quite simple in terms of design complexity.

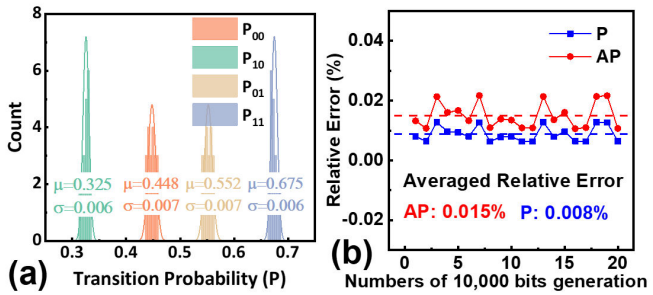

Fig.5. (a) Gaussian distributions of measured transition probabilities with (b) relative error of the final AP state and P state is 0.015% and 0.008%, respectively.

In order to evaluate the measurement error on the transition probabilities themselves, we repeated the 10,000-bit MC signal generation for 20 times, i.e. 200,000 bits in total, and calculated the distribution parameters of each time. As demonstrated in **Fig. 5a**, each transition probability (P_{00}, P_{10}, P_{01} and P_{11}) follows Gaussian distribution. The averaged relative error of AP state and P state is 0.015% and 0.008%, respectively (**Fig. 5b**), which proves that the measurement variability of transition probabilities has an ignorable effect on the quality of the generated MC signal.

Finally, the randomness of the generated MC has been evaluated using the National Institute of Standards and Technology (NIST) Test Suite, a statistical package that evaluates the randomness of binary sequences [27]. As summarized in **Table I**, the 200,000-bit MC signal has passed 12 NIST tests (p-values ≥ 0.001, success proportion ≥ 9/10), supporting the randomness.

TABLE I: NIST TEST RESULT

Test	p-value	Proportion	Result
Frequency	0.534146	9/10	Pass
Block Frequency	0.213309	9/10	Pass
Runs	0.739918	9/10	Pass
Longest Run	0.350485	10/10	Pass
FFT	0.350485	10/10	Pass
Cumulative Sums	0.017912	9/10	Pass
Linear Complexity	0.066882	9/10	Pass
Approximate entropy	0.350485	10/10	Pass
Non- Overlapping Template	0.213309	10/10	Pass
Overlapping Template	0.004301	10/10	Pass
Serial	0.213309	9/10	Pass
Rank	0.534146	10/10	Pass

It should be noted that the good performance of this MTJ-based MC generation solution can be attributed to the intrinsic electron tunneling magneto-resistive effect of MTJ which leads to much better endurance (>10^{14}) and speed (< ns) compared with the RRAM in [16], whose resistive switching relies on the atomic defect movement. Despite this, the proposed MC generation methodology is genetic and applicable to a wider range of emerging memory devices, such as RRAM, phase-change memory (PCRAM), or ferroelectric memory (FeRAM).

IV. CONCLUSIONS

This paper presents a hardware solution for generating MC signals, by using one single MTJ. High quality standard MC signal has been generated with low error and good randomness, based on the industry-ready device and simple waveform. The proposed solution also demonstrates the capability to increase the generation speed in a convenient way. The presented solution offers a hardware-friendly implementation of MC signal in semiconductor chips, especially for emerging applications such as machine learning and encryption.

REFERENCES

[1] P. A Gagniuc, Markov Chains: From Theory to Implementation and Experimentation, Amsterdam: John Wiley & Sons, 2017, doi: 10.1002/9781119387596.

[2] M. Korczynski and A. Duda, "Markov Chain Fingerprinting to Classify Encrypted Traffic," in *IEEE Conference on Computer Communications*, Toronto, ON, Canada, 2014, doi: 10.1109/INFOCOM.2014.6848005.

[3] W.-K. Ching, X. Huang, M. K. Ng, T.-K. Siu, Markov Chains: Models, Algorithms and Applications, Springer Sci. Bus. Media, 2013, doi: 10.1007/0-387-29337-X.

[4] F. Pachet and P. Roy, "Markovian-sequence generator and new methods of generating Markovian sequences". US Patent US8566258B2, 22 10 2013.

[5] Z. Chai, J. Ma, W. Zhang, B. Govoreanu, E. Simoen, J. F. Zhang, Z. Ji, R. Gao, G. Groeseneken and M. Jurczak, "RTN-based defect tracking technique: Experimentally probing the spatial and energy profile of the critical filament region and its correlation with HfO2RRAM switching operation and failure mechanism," in *IEEE Symposium on VLSI Technology*, Honolulu, HI, USA, 2016, doi: 10.1109/VLSIT.2016.7573402.

[6] J. Ma, Z. Chai, W. Zhang, B. Govoreanu, J. F. Zhang, Z. Ji, B. Benbakhti, G. Groeseneken and M. Jurczak, "Identify the critical regions and switching/failure mechanisms in non-filamentary RRAM (a-VMCO) by RTN and CVS techniques for memory window improvement," in *IEEE International Electron Devices Meeting (IEDM)*, San Francisco, CA, USA, 2016, doi: 10.1109/IEDM.2016.7838466.

[7] A. Chimenton, C. Zambelli, P. Olivo, "A New Methodology for Two-Level Random-Telegraph-Noise Identification and Statistical Analysis," *IEEE Electron Device Letters,* vol. 31, no. 6, pp. 612 - 614, 2010, doi: 10.1109/LED.2010.2046311.

[8] S. Vecchi, P. Pavan and F. M. Puglisi, "The Impact of Electrostatic Interactions Between Defects on the Characteristics of Random Telegraph Noise," *IEEE Transactions on Electron Devices,* vol. 12, no. 69, pp. 6991-6998, 2022, doi: 10.1109/TED.2022.3213502.

[9] A. Mohanty, K. B. Sutaria, H. Awano, T. Sato and Y. Cao, "RTN in Scaled Transistors for On-Chip Random Seed Generation," *IEEE Transactions on Very Large Scale Integration (VLSI) Systems,* vol. 8, no. 25, pp. 2248 - 2257, 2017, doi: 10.1109/TVLSI.2017.2687762.

[10] C.-Y. Chen, Q. Ran, H.-J. Cho, A. Kerber, Y. Liu, M.-R. Lin, R. W. Dutton, "Correlation of Id- and Ig-Random Telegraph Noise to Positive Bias Temperature Instability in Scaled High-κ/Metal Gate n-type MOSFETs," in *International Reliability Physics Symposium*, Monterey, CA, 2011, doi: 10.1109/IRPS.2011.5784475.

[11] M. Trabelsi, L. Militaru, A. Savio, S. Monfray and A. Souif, "High-k Gate Stack Properties in SON Transistor Given by Voltage and Temperature Dependence of Random Telegraph Signal," *IEEE Transactions on Electron Devices,* vol. 6, no. 58, pp. 1798 - 1803, 2011, doi: 10.1109/TED.2011.2132722.

[12] W. A. Borders, A. Z. Pervaiz, S. Fukami, K. Y. Camsari, H. Ohno and S. Datta, "Integer factorization using stochastic magnetic tunnel junctions," *Nature,* vol. 573, pp. 390-393, 2019, doi: 10.1038/s41586-019-1557-9.

[13] F. Cai, S. Kumar, T. V. Vaerenbergh, X. Sheng, R. Liu, C. Li, Z. Liu, M. Foltin, S. Yu, Q. Xia, J. J. Yang, R. Beausoleil, W. D. Lu and J. P. Strachan, "Power-efficient combinatorial optimization using intrinsic noise in memristor Hopfield neural networks," *Nature Electronics,* vol. 3, p. 409–418 , 2020, doi: 10.1038/s41928-020-0436-6.

[14] M.-H. Wu, M.-S. Huang, Z. Zhu, F.-X. Liang, M.-C. Hong, J. Deng, J.-H. Wei, S.-S. Sheu, C.-I Wu, G. Liang and T.-H. Hou, "Compact Probabilistic Poisson Neuron Based on Back-Hopping Oscillation in STT-MRAM for All-Spin Deep Spiking Neural Network," in *IEEE Symposium on VLSI Technology*, Honolulu, HI, USA, 2020, doi: 10.1109/VLSITechnology18217.2020.9265033.

[15] X. Zhang, Z. Wang, W. Song, R. Midya, Y. Zhuo, R. Wang, M. Rao, N. K. Upadhyay, Q. Xia, J. J. Yang, Q. Liu and M. Liu, "Experimental Demonstration of Conversion-Based SNNs with 1T1R Mott Neurons for Neuromorphic Inference," in *IEEE International Electron Devices Meeting (IEDM)*, San Francisco, CA, USA, 2019, doi: 10.1109/IEDM19573.2019.8993519.

[16] H. Tian, X.-F. Wang, M. A. Mohammad, G.-Y. Gou, F. Wu, Y. Yang and T.-L. Ren, "A hardware Markov chain algorithm realized in a single device for machine learning," *Nature Comminications,* vol. 9, p. 4305, 2018, doi: 10.1038/s41467-018-06644-w.

[17] R. Beach, T. Min, C. Horng, Q. Chen, P. Sherman, S. Le, S. Young, K. Yang, H. Yu, X. Lu, W. Kula, T. Zhong, R. Xiao, A. Zhong, G. Liu, J. Kan, J. Yuan, J. Chen, R. Tong, J. Chien, T. Torng, D. Tang, P. Wang, M. Chen, S. Assefa, M. Qazi, J. DeBrosse et al., "A statistical study of magnetic tunnel junctions for high-density spin torque transfer-MRAM (STT-MRAM)," in *IEEE International Electron Devices Meeting*, San Francisco, CA, USA, 2008, doi: 10.1109/IEDM.2008.4796679.

[18] R. Carboni, W. Chen, M. Siddik, J. Harms, A. Lyle, W. Kula, G. Sandhu and D. Ielmini, "Random Number Generation by Differential Read of Stochastic Switching in Spin-Transfer Torque Memory," *IEEE Electron Device Letters,* vol. 7, no. 39, pp. 951 - 954, 2018, doi: 10.1109/LED.2018.2833543.

[19] H. Zhao, A. Lyle, Y. Zhang, P. K. Amiri, G. Rowlands, Z. Zeng, J. Katine, H. Jiang, K. Galatsis, K. L. Wang, I. N. Krivorotov and J.-P. Wang, "Low writing energy and sub nanosecond spin torque transfer switching of in-plane magnetic tunnel junction for spin torque transfer random access memory," *Journal of Applied Physics ,* vol. 109, p. 07C720, 2011, doi: 10.1063/1.3556784.

[20] M.-H. Wu, M.-C. Hong, C.-C. Chang, P. Sahu, J.-H. Wei, H.-Y. Lee, S.-S. Sheu and T.-H. Hou, "Extremely Compact Integrate-and-Fire STT-MRAM Neuron: A Pathway toward All-Spin Artificial Deep Neural Network," in *IEEE Symposium on VLSI Technology*, Kyoto, Japan, 2019, doi: 10.23919/VLSIT.2019.8776569.

[21] M. Song, W. Duan, S. Zhang, Z. Chen and L. You, "Power and area efficient stochastic artificial neural networks using spin–orbit torque-based true random number generato," *Applied Physics Letters,* vol. 118, no. 5, p. 052401, 2021, doi: 10.1063/5.0035857.

[22] G. Narasimman, J. Basu, P. Sethi, S. Krishnia, C. Yi, W. S. Lew and A. Basu, "A 126 µW Readout circuit in 65nm CMOS with Successive Approximation Based Thresholding for Domain Wall Magnet Based Random Number Generator," *IEEE Sensors Journal,* vol. 20, no. 14, pp. 7810 - 7818, 2020, doi: 10.1109/JSEN.2020.2980021.

[23] B. R. Zink, Y. Lv and J.-P. Wang, "Telegraphic switching signals by magnet tunnel junctions for neural spiking signals with high information capacity," *Journal of Applied Physics,* vol. 15, no. 124, p. 152121, 2018, doi: 10.1063/1.5042444.

[24] B. R. Zink , Y. Lv, and J.-P. Wang, "Independent Control of Antiparallel- and Parallel-State Thermal Stability Factors in Magnetic Tunnel Junctions for Telegraphic Signals With Two Degrees of Tunability," *IEEE Transactions on Electron Devices,* vol. 12, no. 66, pp. 5353 - 5359, 2019, doi: 10.1109/TED.2019.2948218.

[25] W. F. Brown, "Thermal Fluctuations of a Single-Domain Particle," *Phys. Rev. ,* vol. 130, no. 5, p. 1677, 1963, doi: 10.1103/PhysRev.130.1677.

[26] C. Safranski, G. Hu, J. Z. Sun, P. Hashemi, S. L. Brown, L. Buzi, C. P. D'Emic, E. R. J. Edwards, E. Galligan, M. G. Gottwald, O. Gunawan, S. Karimeddiny, H. Jung, J. Kim, K. Latzko, P. L. Trouilloud, S. Zare, D. C. Worledge, "Reliable Sub-nanosecond MRAM with Double Spin-torque Magnetic Tunnel Junctions," in *IEEE Symposium on VLSI Technology and Circuits (VLSI Technology and Circuits)*, Honolulu, HI, USA, 2022, doi: 10.1109/VLSITechnologyandCir46769.2022.9830306.

[27] A. Rukhin, J. Soto, J. Nechvatal, M. Smid, E. Barker, S. Leigh, M. Levenson, M. Vangel, D. Banks, A. Heckert, J. Dray, and S. Vo, "A statistical test suite for random and pseudorandom number generators for cryptographic applications," NIST, Gaithersburg, MD, USA, 2010.